

On the use of Logistic Regression for stellar classification

An application to colour-colour diagrams

Leire Beitia-Antero · Javier Yáñez · Ana I. Gómez de Castro

Received: XXXX / Accepted: YYYY

Abstract We are totally immersed in the Big Data era and reliable algorithms and methods for data classification are instrumental for astronomical research. Random Forest and Support Vector Machines algorithms have become popular over the last few years and they are widely used for different stellar classification problems. In this article, we explore an alternative supervised classification method scarcely exploited in astronomy, Logistic Regression, that has been applied successfully in other scientific areas, particularly biostatistics. We have applied this method in order to derive membership probabilities for potential T Tauri star candidates from ultraviolet-infrared colour-colour diagrams.

Keywords Methods: statistical - Methods: data analysis - Ultraviolet: stars - Stars: variables: T Tauri, Herbig Ae/Be

1 Introduction

Stellar classification has evolved in leaps and bounds for the last several years. Nowadays, lots of stellar catalogues are available online, with hundreds of thousands of sources, and so machine learning algorithms have become a popular and powerful tool to classify these enormous datasets. One of the commonly-used supervised methods is Random Forest (Breiman (2001)), that has been applied in order to classify variable stars from the Hipparcos sample (Dubath et al (2011); Johnston and Oluseyi (2017); Pichara and Protopapas (2013)) or Kepler catalogue (Bass and Borne (2016)). Another widely used automatic classification algorithm is Support Vector Machines (Cortes and Vapnik (1995); Vapnik (1999); Cristianini and Shawe-Taylor (2000)) that

This work has been partly funded by the Ministry of Economy, Industry and Competitiveness of Spain through grants ESP2014-54243-R, ESP2015-68908-R and TIN2015-66471-P as well as by the local Government of Madrid through grant S2013/ICE2845.

Facultad de Matemáticas, Universidad Complutense de Madrid, Plaza de las Ciencias 3, 28040 Madrid, Spain · AEGORA Research Group, Universidad Complutense de Madrid, Plaza de las Ciencias 3, 28040 Madrid, Spain E-mail: aig@ucm.es

has been applied by [Kurcz et al \(2016\)](#) to the WISE catalogue to obtain star, galaxy and quasar catalogues, and it is also the main algorithm used to classify all the Gaia sources ([Bellas-Velidis et al \(2012\)](#)). There exist other algorithms based on bayesian methods such as those proposed by [Picaud et al \(2005\)](#) or [Bailer-Jones \(2011\)](#) that allow to improve the accuracy of the classification. All these methods are designed to cope with huge amounts of sources and are suited for data with multidimensional nature. However, in some cases the simplicity of the problem or a reduced sample are not worth the effort.

The logistic function was introduced by Verhulst ([Verhulst \(1845, 1847\)](#)) in the 19th century to describe population growth in biological experiments and was early applied on chemical processes ([Reed and Berkson \(1929\)](#)); a later formulation was given by [Cox \(1958\)](#). Currently, Logistic Regression is one of the most used techniques in Biostatistics (see [Hosmer et al \(2013\)](#)). Logistic Regression is a multivariate analysis model that predicts the probability of membership to any class based on the values of some predictor variables; these variables are not constrained to follow a given (normal) distribution, not even be continuous. Although this method is not widely used in astrophysics, it has been recently applied by [Huppenkothen et al \(2017\)](#) in order to study the variability of the galactic black hole binary GRS 1915+105. Moreover, a variation of the method (Boosted Logistic Regression) has been compared with Random Forest by [Saz Parkinson et al \(2016\)](#) to classify gamma-ray sources into two groups and they have shown that similar accuracy is achieved with both methods.

The Galaxy Evolution Explorer (GALEX) mission ([Martin et al \(2005\)](#)) has surveyed the sky in two ultraviolet bands, the far ultraviolet (FUV) band (1344 Å-1786 Å) and the near ultraviolet (NUV) band (1771 Å- 2831 Å). Already decommissioned, during its life time GALEX detected about 200,000 million sources ([Bianchi et al \(2014\)](#)) that together with the 2MASS survey ([Skrutskie et al \(2006\)](#)) provide an incredible wealth of information to study star formation and the interstellar medium in the Galaxy. Some applications to the Taurus and Orion star forming regions can be found in [Gómez de Castro et al \(2015a,b\)](#); [Sánchez et al \(2014\)](#); [Beitia-Antero and Gómez de Castro \(2017\)](#).

In [Gómez de Castro et al \(2015a\)](#) (hereafter GdC2015) several colour-colour diagrams were used to identify T Tauri Stars (TTSs) from the background stellar population. Although the classification method was purely empirical, some areas were identified where reliable candidates should be located but it neither assigned an uncertainty nor a probability of membership to a given class of the candidates. This is a serious drawback to elaborate sensible lists of candidates for subsequent observation. Logistic Regression algorithms model robustly the probability of membership, providing a measure of the classification errors.

In this work, we apply Logistic Regression to the empirical classification done in GdC2015 and show how membership probabilities can be calculated. In Section 2, the method is described and in Section 3 is applied to the sample in GdC2015. In Section 4 results of the application of the algorithm to a sample of Main Sequence stars are shown and the computational details are included in the Appendix. A short summary of the results is provided in Sec. 5.

2 Logistic Regression

Logistic Regression is a machine learning model used to solve supervised classification problems: given a sample of objects characterised by the values of some predictor or independent variables, and knowing the class (dependent variable) of each one, the variables are used to classify the objects in the given groups. The solution of the Logistic Regression model will be a function that, given a new set of values of dependent variables, will compute the probability of belonging to any of the pre-defined classes.

Mathematically, (see for instance [Hastie et al \(2013\)](#) or [Pradhan and Lee \(2010\)](#)), the probability of occurrence of some event, in our case the probability that an object belongs to a particular class or category, is modelled as:

$$p = \frac{1}{1 + \exp(z)} \quad (1)$$

where z is a linear combination of some predictor variables:

$$z = \beta_0 + \beta_1 x_1 + \beta_2 x_2 + \dots + \beta_n x_n \quad (2)$$

The probability p varies from 0 to 1 on an S -shaped curve, β_0 is the intercept of the model and β_i ($i = 1, 2, \dots, n$) are the coefficients of the Logistic Regression model. An appropriate selection of the predictor variables x_1, x_2, \dots, x_n is crucial for an accurate modelling and any combination of the original variables is allowed by the method: $x_j = x_1^2; x_k = x_1 x_2; \dots$

Hence, the classification problem can be expressed as, *Given a set of classes $\{1, 2, \dots, K\}$, and given an astronomical object $o \in \mathcal{O}$ characterised by a set of variables $\mathbf{x}^o = (x_1^o, x_2^o, \dots, x_n^o)$, what is $P(G = k | \mathbf{x}^o)$, the probability that the object belongs to any of these classes?*

The answer will distinguish between the probability of classes $1, 2, \dots, K - 1$ and is given as,

$$P(G = k | \mathbf{x}^o) = \frac{\exp(\beta_{k0} + \sum_{i=1}^n \beta_{ki} x_i^o)}{1 + \sum_{h=1}^{K-1} \exp(\beta_{h0} + \sum_{i=1}^n \beta_{hi} x_i^o)} \quad k \in \{1, 2, \dots, K - 1\} \quad (3)$$

and the probability of class K ,

$$P(G = K | \mathbf{x}^o) = \frac{1}{1 + \sum_{h=1}^{K-1} \exp(\beta_{h0} + \sum_{i=1}^n \beta_{hi} x_i^o)} \quad (4)$$

By definition $\sum_{h=1}^K P(G = h | \mathbf{x}^o) = 1, \forall \mathbf{x}^o$.

The parameters $\{\beta_{k,i}, k = 1, \dots, K, i = 1, \dots, n\}$ are estimated from a qualification sample $\{(x_1^j, \dots, x_n^j), y^j \mid j = 1, \dots, m\}$ where (x_1^j, \dots, x_n^j) are the variables that characterise objects $j, j = 1, \dots, m$ respectively, and $y^j \in \{1, \dots, K\}$ are the classes.

In this type of problems, the *Classification Table* or *Confusion Matrix* is commonly used. This is a square matrix C with dimension K , the number of classes, and such that any element $c_{i,j}$ indicates the number of objects of class i that are classified by the model into class j , for all $i, j \in \{1, 2, \dots, K\}$ (see [Table 1](#)).

Table 1 Classification Table (Confusion Matrix) for K classes

Classified	Predicted			
	<i>Class 1</i>	<i>Class 2</i>	...	<i>Class K</i>
<i>Class 1</i>	$c_{1,1}$	$c_{1,2}$...	$c_{1,K}$
<i>Class 2</i>	$c_{2,1}$	$c_{2,2}$...	$c_{2,K}$
⋮	⋮	⋮	⋮	⋮
<i>Class K</i>	$c_{K,1}$	$c_{K,2}$...	$c_{K,K}$

3 Classification of T Tauri stars

Our scope is to use the Logistic Regression model to assign a given star with known FUV, NUV, J and K magnitudes a probability of being either a classical or weak-line TTS. GdC2015 obtained a qualification sample of 47 TTSs detected in the Taurus molecular cloud that had been observed either by the International Ultraviolet Explorer (Gómez de Castro and Franqueira (1997)) or by GALEX and that have a 2MASS counterpart; that sample consists on 16 weak line TTSs (WTTs) and 31 Classical TTSs (CTTs). As pointed out by GdC2015, though WTTs are close to the main sequence and it is difficult to identify them directly from the diagram, a regression line was found; this was not the case of the CTTs, that were sparsely distributed over an area far from the main sequence. In addition, both groups seem to be mixed. For this reason, the crucial issue in this work is to define properly the location of the Main Sequence in the FUV-NUV versus J-K colour-colour diagram.

3.1 Model 1: Main Sequence defined by the Field Stars in the area

In a first attempt, we used a sample of 7348 stars observed by GALEX in Taurus, with both FUV and NUV magnitudes, that also had a 2MASS counterpart (see GdC2015 for details); this plain sample will be referred to as Field Stars (FS) and is shown in Fig. 1 (red dots). Note that the separation between the WTTs and FS is rather fuzzy due to variations on the extinction values of some FS, and will complicate the differentiation of both classes. Besides, the size of the FS sample is enormous compared to the CTTs and WTTs ones and will bias the results.

The problem will consist on discerning the probability that any of the FS is a CTTs or WTTs (or neither of them, and so they will remain as FS). Following the Logistic Regression formulation (Sec. 2), we will determine the membership probability to any of the three classes: CTTs ($k = 1$), WTTs ($k = 2$) and FS ($k = 3$), where higher probability of belonging to the FS class means that the object is not likely to be a TT. The variables considered are $x_1 = J - K$, $x_2 = FUV - NUV$, $x_3 = x_1^2$, $x_4 = x_2^2$ and $x_5 = x_1 x_2$; variables x_3 , x_4 and x_5 are introduced due to the nonlinear nature of the sample (Fig. 1). The family of parameters to be estimated is:

$$\{\beta_{ki} \mid k \in \{1, 2\}; i \in \{0, 1, 2, \dots, 5\}\} \quad (5)$$

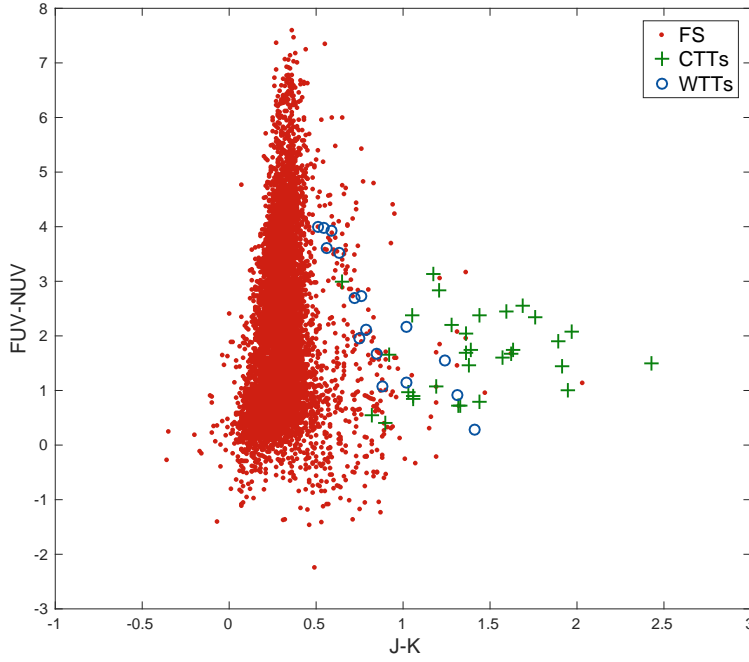


Fig. 1 Initial sample of GALEX field stars (red dots), CTTs (green pluses) and WTTs (blue circles) from GdC2015.

Table 2 Slope coefficients of the quadratic Logistic Regression model for the TT sample. $k = 1$ coefficients correspond to the CTTs population while $k = 2$ fits the WTTs population.

	$\beta_{k,0}$	$\beta_{k,1}$	$\beta_{k,2}$	$\beta_{k,3}$	$\beta_{k,4}$	$\beta_{k,5}$
$k = 1$	-14.1806	15.6095	0.9570	-4.3114	-0.2846	0.4122
$k = 2$	-24.6297	34.0705	4.9589	-12.9391	-0.5180	-2.5460

where $k = 1$ corresponds to the first class, CTTs, and $k = 2$ corresponds to the second class, WTTs. A computational application was programmed in MATLAB ([MathWorks \(2014\)](#)) to estimate the parameters as well as to obtain the associated graphics. The results are given in Table 2.

In Fig. 2, the most likely class for each point of the (J-K)-(FUV-NUV) plane has been determined from the Logistic Regression results (coloured mesh grid corresponds to the colour code of the sample: blue for WTTs, green for CTTs and red for FS). As occurs with every automated classification procedure, we find misclassified objects among our sample (mainly the WTTs population, that has been ignored) that should be minimum if the algorithm behaves properly. The contours delimit the areas inside which the membership probability is higher to 0.5 (solid line), 0.8 (dashed line) and 0.9 (dotted line). Note that given the definition of the probabilities (Eqs. 3 and 4) and the fact that we are establishing three groups, the areas of, e.g. $P \geq 0.5$, may

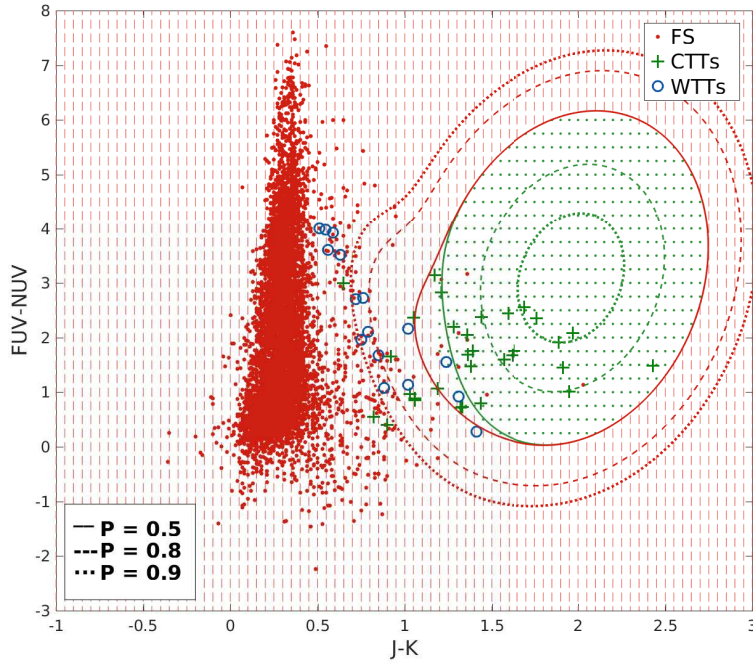


Fig. 2 Results of the Logistic Regression fit of the FS and TTs sample from GdC2015. Each point of the plane has been assigned the most probable class with a color code: vertical red lines for FS and green points for CTTs. Also three probability lines have been plotted in order to separate the 0.5, 0.8 and 0.9 probability regions for FS (red) and CTTs (green). The algorithm has ignored the WTTs class.

not be closed areas but rather open ones, as happens with the FS sample. As mentioned above, virtually no point has been assigned to WTTs class. This is positively due to a lack of balance in the sample as the most numerous population corresponds to FS whereas the WTTs sample is the least populated. Moreover, FS are submitted to different extinctions resulting in a broadening of the MS branch and as WTTs lie pretty near of the FS population, the algorithm is obviously confusing both classes. The discouraging results of the confusion matrix (see Table 3) support this fact.

Table 3 Confusion Matrix for Model 1: initial unbalanced sample.

Classified	Predicted		
	<i>CTTS</i>	<i>WTTs</i>	<i>FS</i>
<i>CTTS</i>	19	0	12
<i>WTTs</i>	2	0	14
<i>FS</i>	9	0	7339

Hence, it is necessary to compensate the sample in order to achieve better results.

Table 4 Slope coefficients of the quadratic Logistic Regression model for the TT balanced sample using the upper limits for the scaling coefficients, $\lambda_1 = 237, \lambda_2 = 459$.

	$\beta_{k,0}$	$\beta_{k,1}$	$\beta_{k,2}$	$\beta_{k,3}$	$\beta_{k,4}$	$\beta_{k,5}$
$k = 1$	-9.1677	17.8639	-2.6685	-7.2559	0.0526	4.4272
$k = 2$	-24.9926	39.4334	6.2785	-14.5633	-0.7100	-1.8300

3.2 Model 2: Main sequence from a balanced sample of field stars.

As we will show below, the best solution is achieved by reducing the statistical weight of field stars. From a statistical point of view, it is sensible to have equal probability of belonging to any of the three classes (CTTS, WTTS or other, FS), supposing the sample is a simple random one. Given the fact that the FS population is much numerous than the TTs population, the algorithm could ignore the WTTs without a significant penalty on the results, as we have shown in the first approach. A possible solution for this problem is to balance the CTTS and WTTs sample sizes by integer factors λ_1 and λ_2 , respectively, in order to obtain more flexible probability distributions that fit better to the spatial distribution of the sources. An upper limit for these parameters is established by the size of the FS sample (7348), *i.e.*, $\lambda_1 = 7348/31 \sim 237$ and $\lambda_2 = 7348/16 \sim 459$. If we perform again the Logistic Regression using these upper limits (see Table 4 for the slope coefficients), the results are highly improved as clear from Fig. 3, in the sense that the WTTs class has not been ignored and most of the sources lie inside their $P > 0.5$ probability area.

Formally, this improvement can be tracked through the Rate matrix, R . R is a $K \times K$ matrix with elements $r_{i,j}$ defined as the fraction of the total sources belonging to class i that have been classified as class j , where $i, j \in \{1, 2, \dots, K\}$ ($K = 3$ in this case). This matrix is similar to the confusion matrix in that the classification improves as the elements outside the main diagonal decrease toward 0. The rate matrix for model 1 (see Sec. 3.1) is,

$$R = \begin{pmatrix} 0.61 & 0.00 & 0.39 \\ 0.12 & 0.00 & 0.88 \\ 0.00 & 0.00 & 1.00 \end{pmatrix}$$

that shows clearly that the FS class is overestimated. However, for the scaled model considering $\lambda_1 = 237, \lambda_2 = 459$, the rate matrix is:

$$R = \begin{pmatrix} 0.74 & 0.26 & 0.00 \\ 0.12 & 0.88 & 0.00 \\ 0.01 & 0.02 & 0.97 \end{pmatrix}$$

The case $R = I$, the identity matrix, will correspond to the perfect classification, where the predicted class of every source will be the real one. The difference between matrices R and I can be considered a quality measure of the classification algorithm. The final step is to determine λ_1 and λ_2 values in order to improve as much as possible this rate matrix R . These integer values should be in the ranges $\lambda_1 \in \{1, \dots, 237\}$ and

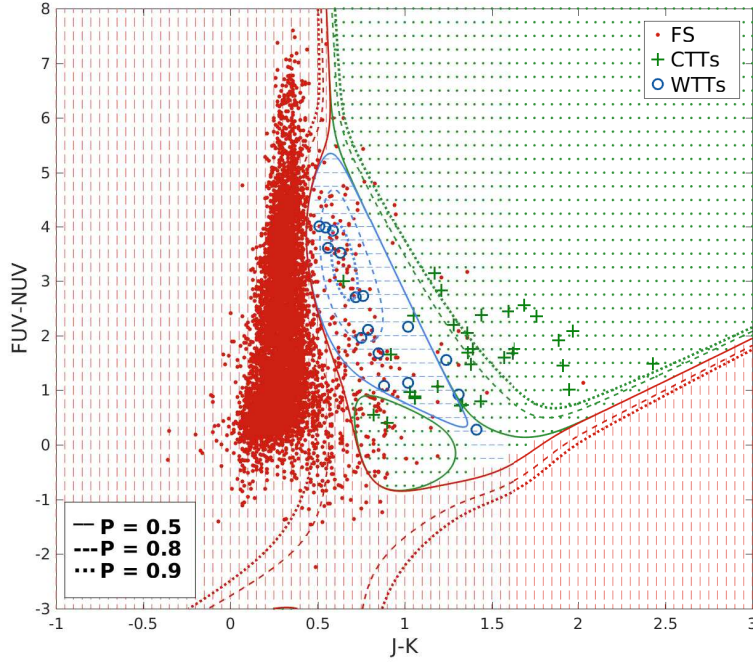


Fig. 3 Results of the Logistic Regression fit with a sample balanced using the upper limits for the scaling coefficients, $\lambda_1 = 237, \lambda_2 = 459$. Some points of the plane has been assigned to the WTTs class (blue horizontal lines). Also three probability lines have been plotted in order to separate the 0.5, 0.8 and 0.9 probability regions.

$\lambda_2 \in \{1, \dots, 459\}$. After several experiments, we have found that the best values in the sense of the matrix $R - I$ are $\lambda_1 = 69, \lambda_2 = 86$, providing the confusion matrix showed in table 5 and rate matrix,

$$R = \begin{pmatrix} 0.94 & 0.06 & 0.00 \\ 0.19 & 0.81 & 0.00 \\ 0.01 & 0.01 & 0.98 \end{pmatrix}$$

Table 5 Confusion Matrix for the model considering a balanced sample, with $\lambda_1 = 69, \lambda_2 = 86$.

Classified	Predicted		
	CTTS	WTTs	FS
CTTS	29	2	0
WTTs	3	13	0
FS	54	96	7198

Table 6 Slope coefficients of the quadratic Logistic Regression model for the TT balanced sample using the set values for the scaling coefficients, $\lambda_1 = 69, \lambda_2 = 86$.

	$\beta_{k,0}$	$\beta_{k,1}$	$\beta_{k,2}$	$\beta_{k,3}$	$\beta_{k,4}$	$\beta_{k,5}$
$k = 1$	-10.7245	18.1355	-1.6004	-6.8158	-0.1001	3.7088
$k = 2$	-25.0890	38.4523	5.8147	-14.1837	-0.6552	-1.7137

Table 7 Membership probability for TTs candidates^(a) selected by GdC2015 in the Taurus region. The results correspond to the balanced Logistic Regression model with $\lambda_1 = 69$ and $\lambda_2 = 86$. The full table is available as online material.

RA (deg)	Dec (deg)	FUV (mag)	NUV (mag)	J (mag)	K (mag)	Type ^a	P(CTTs)	P(WTTs)	P(FS)
60.176	28.871	20.21	17.87	11.17	10.58	Candidate	0.0808	0.5311	0.3881
61.042	29.337	21.77	17.9	9.57	8.92	Candidate WTTS	0.0712	0.8435	0.0852
61.498	29.944	20.85	17.68	10.19	8.83	Candidate CTTS	0.9970	0.0030	0.000
62.06	21.632	21.81	20.93	9.46	8.66	Candidate	0.4637	0.2679	0.2684
62.065	30.262	21.37	20.75	13.86	13.02	Candidate	0.5155	0.2019	0.2826
62.269	28.923	21.75	18.17	9.96	9.36	Candidate WTTS	0.0415	0.7995	0.1590
63.463	28.761	21.51	18.68	10.99	10.45	Candidate	0.0342	0.5140	0.4518
64.222	26.405	16.76	16.12	13.21	12.35	Candidate	0.5285	0.2357	0.2358
64.716	23.858	20.9	19.19	11.29	10.58	Candidate	0.2441	0.5539	0.2020
64.760	31.765	20.97	17.39	10.4	9.84	Candidate WTTS	0.0271	0.7075	0.2654

The results are shown in Fig 4. This time there are some regions of the plane where the membership probability to WTTs class is non-zero and greater than 0.5 and the majority of the WTTs population lies; the slope coefficients are listed in Table 6. With these parameters, we have assigned a membership probability to all TTSs candidates¹; they are listed in Table 7 and represented in Fig. 4 as black crosses. It is clear from the plot that there are many FS lying inside the $P > 0.8$ areas of WTTs and CTTs that were not selected as likely candidates to TTs by GdC 2015. We want to highlight that statistical methods are useful to derive probability distributions but as intrinsic variations inside the sample are not considered, plenty of objects might be misclassified. GdC2015 performed a careful examination of the FS sample and even analysed the spectral energy distribution curves of some of the sources in order to elaborate a reduced but clean sample of TTs candidates. Thus, the combination of both methodologies is instrumental to achieve reliable results.

4 On the possibility of Main Sequence definition from spectroscopic data

An additional approach, which is worth exploring, is to define the main sequence (MS) from spectroscopic observations as has been done for the TTSs. Our qualification sample has been extracted from the high quality photometric catalogue derived by Beitia-Antero and Gómez de Castro (2016) (hereafter BAGdC) using IUE spectra. We selected sources from BAGdC's catalogue with both FUV and NUV synthetic

¹ As a reminder, GdC2015 labeled the potential TTS as *Candidate WTTS*, *Candidate CTTS* or just *Candidate* if it was not clear to which class the star might belong to. Logistic Regression allows us to assign a membership probability to those objects. in GdC2015's Taurus survey to select in the future the best ones for follow up observations and subsequent characterisation

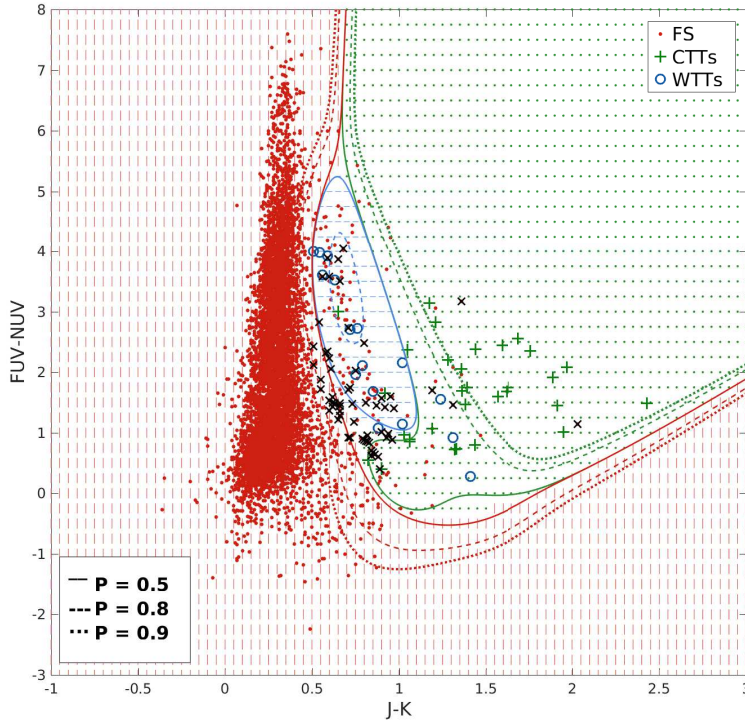


Fig. 4 Results of the Logistic Regression fit with a sample balanced using the selected values of the scaling coefficients, $\lambda_1 = 69, \lambda_2 = 86$. The plane seems to be well organised in three different regions assigned to each of the three classes, FS, WTTs and CTTs. Some probability lines have been plotted in order to separate the 0.5, 0.8 and 0.9 probability regions. Black crosses correspond to the TTs candidates selected by GdC2015.

magnitudes and cross-correlated the results with the 2MASS catalogue (Skrutskie et al (2006)) in a search radius of $3''$ to obtain J and K magnitudes; the spectral types were retrieved from the SIMBAD database (Wenger et al (2000)). Unfortunately, only B and A spectral types had a representative number of sources (we found less than five stars with O, F, G or K spectral type); also sdO and sdB populations were numerous enough. Details of the final sample are listed in Table 8.

Table 8 IUE sample of MS and sub-dwarf stars with synthetic FUV and NUV magnitudes from BAGdC and J and K magnitudes from 2MASS. Spectral types were retrieved from SIMBAD.

Spectral type	B,BV	A,AV	sdO	sdB
Stars	51	26	17	8

Due to the poverty of the sample we have not been able to characterise the MS population as precisely as needed in order to distinguish it from the young stellar objects. The details of the calculation can be found in the Appendix (Sec. 6).

5 Conclusions

In this article we have shown that Logistic Regression, a mathematical tool seldom used in astronomy, can be implemented in classification problems. The algorithm has been applied to assign a probability of being a T Tauri star from FUV-NUV versus J-K colour-colour diagrams. This methodology, combined with a careful qualitative analysis of the diagrams (as in GdC2015), provides potential candidates to for further scrutiny. Both observational and statistical analysis should be carried out together since the method has proven to be very dependent on the shape and size of the sample. In this manner, once a sample of candidates has been selected according its properties from colour-colour- diagrams, Logistic Regression can be applied in order to obtain a membership probability distribution.

6 Appendix

Provided the poverty of the initial sample of MS stars (see Sec. 4), we decided to combine the four classes into two big groups: MS stars (B and A classes) and sub-dwarfs (sdO and sdB); the spatial distribution of the sources in the $x_1 = \text{J-K}$ vs $x_2 = \text{FUV-NUV}$ plane is shown in Fig. 5. In a natural way, the stars are confined in a subregion of the whole plane \mathbb{R}^2 , so it is coherent to define a smaller area or feasible region that is expected to contain the vast majority of the sources and that facilitates the obtention of more accurate results; in this case, it has been defined as $-0.6 \leq \text{J} - \text{K} \leq 0.7$ and $-0.8 \leq \text{FUV} - \text{NUV} \leq 1.8$. This subspace has been further divided by adjusting the sequence of A and B stars following a third degree equation that passes through four simulated points (see Fig. 5): $x_2 = 0.97 + 11.42 \cdot x_1 + 42.81 \cdot x_1^2 + 57.08 \cdot x_1^3$. Once all these assumptions were made, we dropped from the sample the two points that were out of the feasible region as well as other MS stars that showed abnormally infrared excesses.

6.1 Logistic Regression - Application to two classes

In this case, the classification problem consists on distinguishing between two classes ($K = 2$): AB ($k = 1$) and sd ($k = 2$). Therefore, given one of these objects O the problem reduces to determine the probability of belonging to the first class, AB :

$$P(AB|\mathbf{x}^o) = \frac{\exp(f(x))}{1 + \exp(f(x))} \doteq p_1 \quad (6)$$

and so, the probability of membership to the sd class is:

$$P(sd|\mathbf{x}^o) = 1 - P(AB|\mathbf{x}^o) = 1 - p_1 = \frac{1}{1 + \exp(f(x))} \doteq p_2 \quad (7)$$

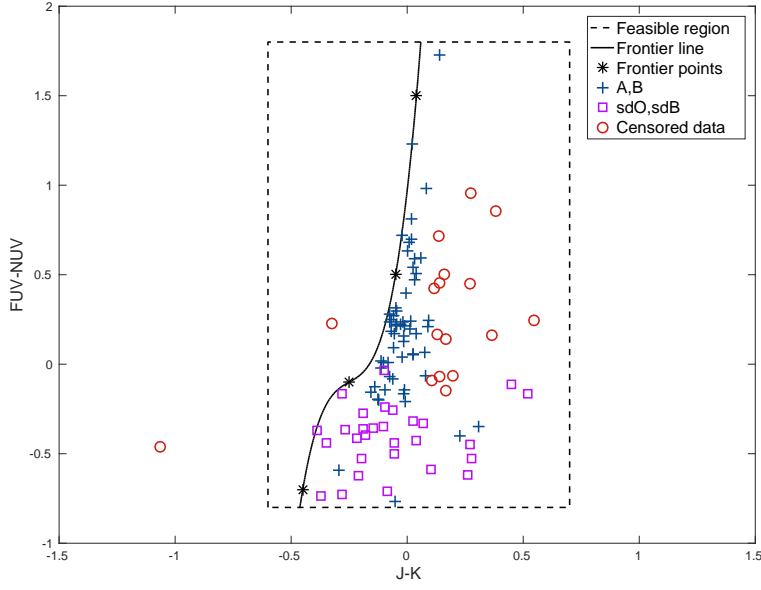


Fig. 5 Spatial distribution of the MS stars in the (J-K)-(FUV-NUV) plane. Most of the sources lie inside the feasible region and at the right of the predefined cubic curve. MS class is represented by + while sub-dwarf class is represented by open squares. Censored data are represented with open circles (see text).

The independent variables of the regression model are in a natural way $x_1 = J - K$ and $x_2 = FUV - NUV$. It is clear in Fig. 5 that the classification cannot be linear and so, after some computational experience, the variables have been extended to $x_3 = x_1^2$, $x_4 = x_2^2$ and $x_5 = x_1 x_2$ to perform a quadratic Logistic Regression. Thus, the linear combination of the predictor variables is given by

$$f(x) = \beta_{1,0} + \beta_{1,1}x_1 + \beta_{1,2}x_2 + \beta_{1,3}x_3 + \beta_{1,4}x_4 + \beta_{1,5}x_5 = \beta_{1,0} + \beta_{1,1}x_1 + \beta_{1,2}x_2 + \beta_{1,3}x_1^2 + \beta_{1,4}x_2^2 + \beta_{1,5}x_1x_2 \quad (8)$$

The parameters are listed in Table 9.

Table 9 Slope coefficients of the quadratic Logistic Regression model for the MS sample, that corresponds to the AB class ($k = 1$).

$\beta_{1,0}$	$\beta_{1,1}$	$\beta_{1,2}$	$\beta_{1,3}$	$\beta_{1,4}$	$\beta_{1,5}$
1.9343	1.3240	9.9596	-14.9457	9.9011	-0.9324

Using these results, we have plotted as a guidance the probability lines for $p_1 = 0.5$, $p_1 = 0.9$ and $p_1 = 0.1$ over the original data (Fig. 6). The two populations are fairly separated and more than half of the AB points lie inside the 0.9 probability region.

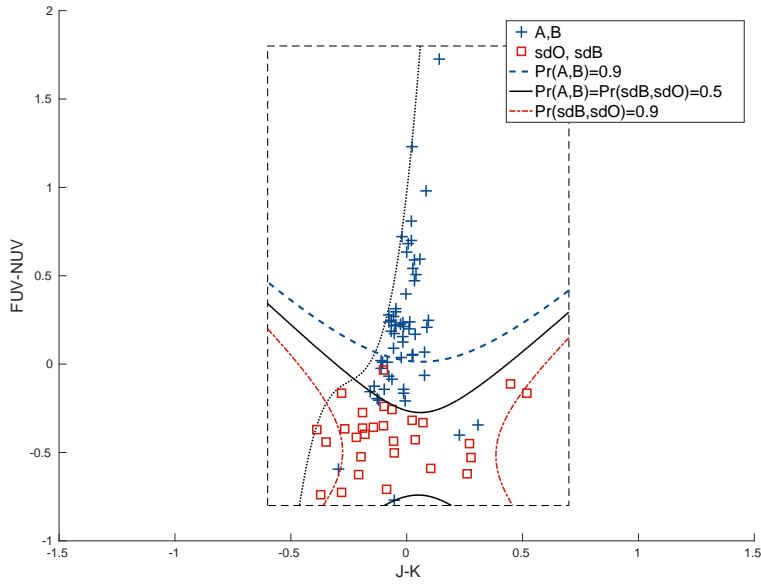


Fig. 6 Probability lines for the MS sample. The solid black line indicates the region of equal probability between *AB* and *sd* classes; the dashed blue (dashed-dotted red) line limits the region of 0.9 probability of belonging to the *AB* (*sd*) class.

The object classification in this framework is made in a simple and natural way: an object O belongs to the *AB* class if $P(O \in AB | \mathbf{x}^o) > P(O \in sd | \mathbf{x}^o)$, where the probabilities are given by Eqs. 6, 7. The ideal situation would be that where both probabilities are the same, that is to say, $p_1 = 0.5$; the confusion matrix is shown in Table 10.

Table 10 Confusion matrix for *MS* and *sd* stars, taking $p_1 = 0.5$.

Classified	Predicted	
	<i>AB</i>	<i>sd</i>
<i>AB</i>	55	3
<i>sd</i>	2	27

Nevertheless, the variable nature of the data suggests that a better classification may be achieved, in the sense that the confusion matrix could be improved to get a minimum number of misclassified objects. We have tested several values for the p_1 parameter, among which are $p_1 = 0.487$, $p_1 = 0.474$ and $p_1 = 0.462$ (see their confusion matrices in Table 11) and found that an acceptable result is achieved with $p_1 = 0.474$. Graphically (see Fig. 7), the vast majority of the data are well classified except for three B stars, PG 1210+429, BD-13 4920 and CSI+81-09137, that

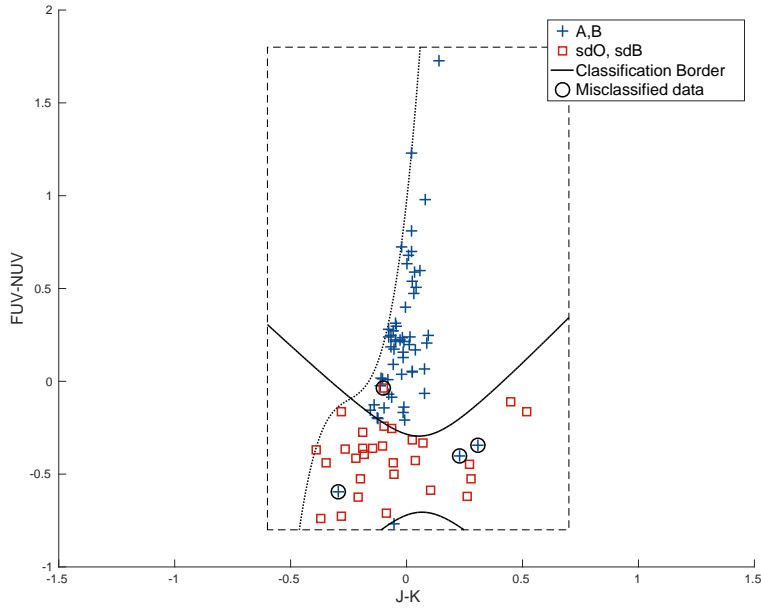


Fig. 7 Best classification of the MS population after applying the Logistic Regression. The line that separates the two classes corresponds to a probability of belonging to the *AB* class of $p_1 = 0.474$ with a 4.6% probability of misclassification.

lie among the *sd* population and one *sdO* star, PG 2219+094, located among the *AB* population. The quality of this classification is also supported by the excellent results obtained for the area under the *Receiver Operating Characteristic* (ROC) curve (see Fig. 8), *AUC*, for the positive condition for MS and *sd* classes; in both cases $AUC = 0.9645$. ROC curve represents the probability of detecting the true condition versus the probability of detecting the false condition, and thus it is restricted to the plane $[0, 1] \times [0, 1]$. *AUC* has become a standard for evaluating classification procedures; the greater the values under the curve, the better the classification.

Table 11 Confusion matrices for several values of p_1 .

Clas.	Pred.	
	<i>AB</i>	<i>sd</i>
<i>AB</i>	53	5
<i>sd</i>	1	28
$p_1 = 0.487$		

Clas.	Pred.	
	<i>AB</i>	<i>sd</i>
<i>AB</i>	55	3
<i>sd</i>	1	28
$p_1 = 0.474$		

Clas.	Pred.	
	<i>AB</i>	<i>sd</i>
<i>AB</i>	55	3
<i>sd</i>	2	27
$p_1 = 0.462$		

To sum up, an object of the MS population is classified as part of the *AB* class if $p_1 \geq 0.474$, and of the *sd* class in another case, with a 4.6% probability of misclassification.

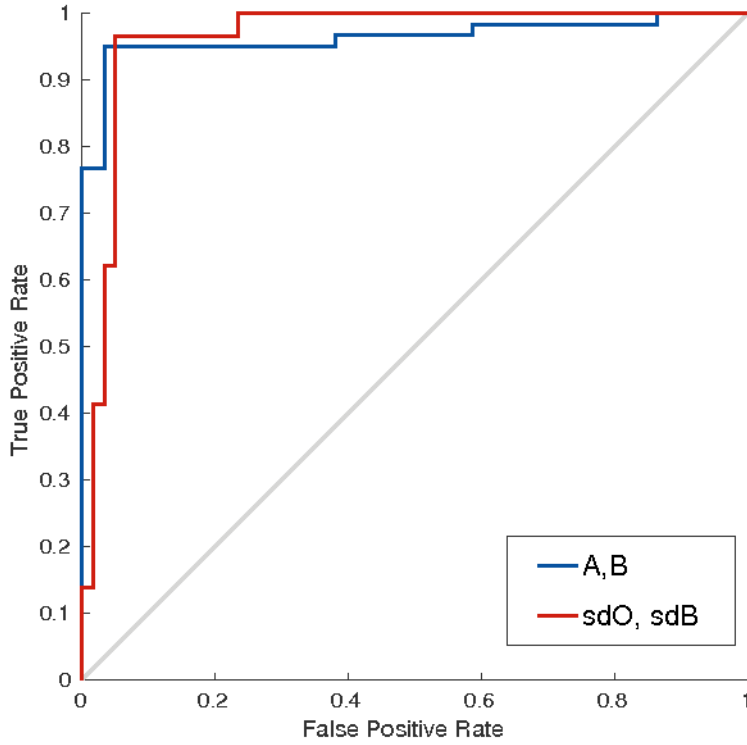


Fig. 8 ROC curve for the final classification of the MS population (TPR vs. FPR), considering $P(AB|x^o) = 0.474$. The blue line corresponds to the AB class, whereas the green line corresponds to the sd class.

Acknowledgements We would like to thank the referee for her/his useful comments that have improved the article.

References

- Bailer-Jones C (2011) Bayesian inference of stellar parameters and interstellar extinction using parallaxes and multiband photometry. *MNRAS* 411:435–452
- Bass G, Borne K (2016) Supervised Ensemble Classification of Kepler Variable Stars. *MNRAS* 459:3721–3737
- Beitia-Antero L, Gómez de Castro AI (2016) A data base of synthetic photometry in the GALEX ultraviolet bands for the stellar sources observed with the International Ultraviolet Explorer. *A&A* 596:A49
- Beitia-Antero L, Gómez de Castro AI (2017) Interstellar extinction in Orion: variation of the strength of the ultraviolet bump across the complex. *Monthly Notices of the Royal Astronomical Society* 469:253
- Bellas-Velidis I, Kontizas M, Dapergolas A, Livanou E, Kontizas E, et al (2012) Unresolved Galaxy Classifier for ESA/Gaia mission: Support Vector Machines approach. *BlaAJ* 18(2):3
- Bianchi L, Conti A, Shiao B (2014) The ultraviolet sky: An overview from the GALEX surveys. *AdSpR* 53(6):900–912
- Breiman L (2001) Random forests. *Machine Learning* 45(1):5–32

- Gómez de Castro A, Lopez-Santiago J, López-Martínez F, Sánchez N, Sestito P, et al (2015a) A Galex-based search for the sparse young stellar population in the TaurusAurigae star forming region. *ApJS* 216:26
- Gómez de Castro AI, Franqueira M (1997) Accretion and UV Variability in BP Tauri. *The Astrophysical Journal* 482:465
- Gómez de Castro AI, López-Santiago J, López-Martínez F, Sánchez N, de Castro E, et al (2015b) Variation of the ultraviolet extinction law across the Taurus-Auriga star-forming complex. a GALEX based study. *Montly Notices of the Royal Astronomical Society* 449:3867–3878
- Cortes C, Vapnik V (1995) Support-Vector Networks. *Machine Learning* 20:273–297
- Cox D (1958) The Regression Analysis of Binary Sequences. *Journal of the Royal Statistical Society Series B (methodological)* 20:215
- Cristianini N, Shawe-Taylor J (2000) *An Introduction to Support Vector Machines: and other Kernel-based learning methods*. Cambridge University Press
- Dubath P, Rimoldini L, Suveges M, Blomme J, López M, et al (2011) Random forest automated supervised classification of Hipparcos periodic variable stars. *MNRAS* 414:2602–2617
- Hastie T, Tibshirani R, Friedman J (2013) *The Elements of Statistical Learning: Data Mining, Inference and Prediction*. Springer Series in Statistics
- Hosmer D, Lemeshow S, Sturdivant X (2013) *Applied Logistic Regression*, 3rd edn. John Wiley and Sons
- Huppenkothen D, Heil L, Hogg D, Mueller A (2017) Using machine learning to explore the long-term evolution of GRS 1915+105. *MNRAS* 466:2364
- Johnston K, Oluseyi H (2017) Generation of a supervised classification algorithm for time-series variable stars with an application to the LINEAR dataset. *NewA* 52:35–47
- Kurcz A, Bilicki M, Solarz A, Krupa M, Pollo A, et al (2016) Towards automatic classification of all WISE sources. *A&A* 592:A25
- Martin D, Fanson J, Schiminovich D, Morrisey P, Friedman P, et al (2005) The Galaxy Evolution Explorer: A Space Ultraviolet Survey Mission. *The Astrophysical Journal* 619:L1
- MathWorks (2014) *MATLAB*. The MathWorks Inc., Natick, MA, USA
- Picaud S, Robin A, Bastian U (2005) A bayesian classification algorithm for gaia. In: Turon C, O’Flaherty K, Perryman M (eds) *The Three-Dimensional Universe with Gaia*, ESA Special Publication, vol 576, p 467
- Pichara K, Protopapas P (2013) Automatic classification of variable stars in catalogs with missing data. *ApJ* 777
- Pradhan B, Lee S (2010) Delineation of landslide hazard areas on Penang Island, Malaysia, by using frequency ratio, logistic regression, and artificial neural network models. *EES* 60:1037–1054
- Reed L, Berkson J (1929) The application of the logistic function to experimental data. *Journal of Physical Chemistry* 33(5):760–779
- Sánchez N, Gómez de Castro AI, López-Martínez F, López-Santiago J (2014) Young Stellar Object candidates toward the Orion region selected from GALEX. *A&A* 572
- Saz Parkinson P, Xu H, Yu P, Salvetti D, Marelli M, et al (2016) Classification and ranking of the FERMI LAT gamma-ray sources from the 3FGL catalog using machine learning techniques. *ApJ* 820:8
- Skrutskie M, Cutri R, Stiening R, Weinberg M, Schneider S, et al (2006) The Two Micron All Sky Survey 2MASS. *AJ* 131:1163–1183
- Vapnik V (1999) An Overview of Statistical Learning Theory. *IEEE Transactions on Neural Networks* 10:988
- Verhulst PF (1845) *Reserches mathématiques sur la loi d’accroissement de la population*. *Nouveaux Mémoires de l’Académie Royale des Sciences, des Lettres et des Beaux-Arts de Belgique* 18:1–38
- Verhulst PF (1847) *Deuxième mémoire sur la loi d’accroissement de la population*. *Nouveaux Mémoires de l’Académie Royale des Sciences, des Lettres et des Beaux-Arts de Belgique* 20:1–32
- Wenger M, Ochsenbein F, Egret D, Dubois P, Bonnarel F, et al (2000) The SIMBAD astronomical database. The CDS reference database for astronomical objects. *A&AS* 143:9–22